Superhydrophobic surfaces from surface-hydrophobized cellulose fibers with stearoyl groups

ARTICLE *in* CELLULOSE · FEBRUARY 2014

Impact Factor: 3.57 · DOI: 10.1007/s10570-014-0505-y

Cellulose (2015) 22:289–299
DOI 10.1007/s10570-014-0505-y

ORIGINAL PAPER

Superhydrophobic surfaces from surface-hydrophobized cellulose fibers with stearoyl groups

Yonggui Wang · Xiang Wang · Lars-Oliver Heim · Hergen Breitzke · Gerd Buntkowsky · Kai Zhang

Received: 1 September 2014 / Accepted: 11 November 2014 / Published online: 18 November 2014

Abstract In this report, surface-hydrophobized cellulose fibers by stearoyl groups were used for the construction of superhydrophobic surfaces. The product after the synthesis contains two components: cellulose microfibers as the major component and nanoscaled segments in small amounts. The crystalline structure of cellulose was maintained after surface modification based on solid-state ^{13}C NMR spectroscopy. Superhydrophobic surfaces showing static water contact angles of >150° were fabricated using freshly prepared products containing both components via the facile route, e.g., solvent casting. The cellulose types, microcrystalline cellulose or cotton linter cellulose fibers, did not significantly affect the chemical modification of cellulose fibers, but the superhydrophobic surfaces using surface-hydrophobized cotton linters as starting materials exhibited higher surface hydrophobicity and better impact stability in comparison to shorter microcrystalline cellulose. Due to the presence of a crystalline cellulose skeleton, the obtained superhydrophobic surfaces are stable during the heat treatment at 80 °C.

Keywords Cellulose fiber · Stearoyl ester · Superhydrophobic · Contact angle

Y. Wang · K. Zhang (✉)
Ernst Berl Institute for Chemical Engineering and Macromolecular Science, Technische Universität Darmstadt, Alarich-Weiss-Str. 8, 64287 Darmstadt, Germany
e-mail: zhang@cellulose.tu-darmstadt.de

X. Wang · L.-O. Heim
Center of Smart Interfaces, Technische Universität Darmstadt, Alarich-Weiss-Straße 10, 64287 Darmstadt, Germany

H. Breitzke · G. Buntkowsky
Eduard-Zintl-Institute for Inorganic Chemistry and Physical Chemistry, Technische Universität Darmstadt, Alarich-Weiss-Straße 4, 64287 Darmstadt, Germany

Introduction

Superhydrophobic surfaces have been under investigation for more than a decade because of their potential wide applications (Barthlott and Neinhuis 1997; Gao and Jiang 2004; Feng et al. 2002). A superhydrophobic surface generally exhibits a water contact angle of >150° and low contact angle hysteresis. An appropriate combination of surface chemistry and surface structure is critical for the fabrication of superhydrophobic surfaces (Feng and Jiang 2006; Feng et al. 2002). A number of materials have been used for this purpose, ranging from perfluorinated polymers (Deng et al. 2012; Dorrer and Rühe 2008; Genzer and Efimenko 2000) to hydrophobic synthetic polymers (Erbil et al. 2003) to inorganic compounds (Guo et al. 2005; Azimi et al. 2013).

In recent years, increasing research interest has focused on the use of naturally occurring sustainable

materials including cellulose composed of β-1,4-linked anhydroglucose units (AGUs). This is not only due to its abundance in nature and sustainable character, but also its advantageous nontoxicity and biocompatibility, which allows wide application opportunities (Klemm et al. 2005; Clift et al. 2011; Malmström and Carlmark 2012; Jin et al. 2012). For example, such superhydrophobic surfaces based on cellulose-derived materials can be used to inhibit bacterial adhesion (Jin et al. 2012).

To avoid a complex chemical modification procedure, surfactants can be used to obtain cellulose whiskers with hydrophobic surfaces (Heux et al. 2000). A recent development has described an elegant modification of cellulosic fibers via solvent-vaporized controllable crystallization of stearic acid in the porous structure of cellulose to fabricate a novel, highly hydrophobic cellulose composite film (He et al. 2013). However, the aforementioned methods rely on the physical adsorption of specific molecules, and as-prepared cellulose-based materials are potentially more labile than those constructed by covalent bonds. Very often, the cellulose fiber itself is the focus of the (super)hydrophobization, and the cellulose substrates themselves are transformed into (super)hydrophobic ones (Song and Rojas 2013). Chemical surface modifications of cellulose fibers were generally conducted using materials with low surface energy, including perfluorocarbons and hydrophobic synthetic polymers (Cunha et al. 2007; Nystrom et al. 2006; Li et al. 2010). Perfluorinated compounds are used because of their highly water-resistant property, such as perfluoroalkyl chains, pentafluorobenzoyl chloride or 1,1,2,2-perfluorooctyl trimethoxysilane (Cunha et al. 2007; Simončič et al. 2013; Vasiljević et al. 2012; Jin et al. 2012; Li et al. 2007). Cellulose nanocrystal (CNCs) modification with palmitoyl chloride vapors during a gas-phase esterification process was carried out to confer a hydrophobic character to the cellulose surface (Berlioz et al. 2009). In addition, stearate and palmitate of nanocellulose were synthesized after surface modification by acid chloride (Vuoti et al. 2013). They formed films after casting from an acetone suspension, and the contact angles were very low (<90°), which was probably because of the smooth surface. Recently, grafting of cellulose fibers with hydrophobic synthetic polymers was developed (Malmström and Carlmark 2012), e.g., using polystyrene (Roy et al. 2005), fluorinated poly(glycidyl methacrylate) (Nystrom et al. 2006) or polyalkylcyanoacrylate (Bayer et al. 2011). Another approach is the decoration of the cellulose fiber surface with inorganic particles, which form desired nano-/microstructures for the superhydrophobicity, e.g., SiO_2 nanoparticles or diamond-like carbon with or without subsequent hydrophobizations (Caschera et al. 2013; Xu and Cai 2008; Yu et al. 2007). However, these approaches generally require the application of volatile or particular chemicals, harsh reaction conditions or special equipment (Song and Rojas 2013; Malmström and Carlmark 2012).

Herein, the fabrication of superhydrophobic surfaces using surface-hydrophobized cellulose fibers by stearoyl groups was investigated in order to expand the use of sustainable materials for tuning surface wettability of other target substrates. The surface-hydrophobized cellulose fibers were prepared after the modification of cellulose fibers with stearoyl chloride under heterogeneous conditions. The chemical and crystalline structures of the obtained products were elucidated using elemental analysis, FT Raman and solid-state ^{13}C NMR spectroscopy. Surface-hydrophobized cellulose fibers solely or together with polystyrene were further used for superhydrophobic surfaces via facile fabrication, such as solvent casting. The surface properties were characterized regarding the morphology, static/receding/advancing contact angles, drop impact and thermostability.

Experimental

Materials

Microcrystalline cellulose (MCC) with granule size of 50 μm, cotton linter cellulose fibers and stearoyl chloride (90 %) were bought from Sigma-Aldrich (Steinheim, Germany). Dry pyridine, ethyl acetate and dichloromethane were received from VWR International GmbH (Darmstadt, Germany). Deionized water (DI water) was used in all experiments. Other chemicals were all of analytical grade and used as received.

Synthesis of surface-hydrophobized cellulose fibers

Cellulose fibers with surface-attached stearoyl groups (CFS) were prepared according to the synthesis reported before with a few modifications (Vaca-Garcia et al. 2003). In a typical case, 1 g cellulose (microcrystalline

cellulose or cotton linters) was washed with methanol to remove traces of moisture before it was suspended in 30 ml pyridine. The mixture was heated up to 100 °C, and 1.54 ml stearoyl acid chloride (2/3 mol stearoyl chloride per mol anhydroglucose units of cellulose) was dropped into the hot cellulose suspension under stirring while the system was purged with nitrogen. After 1 h stirring at 100 °C, the hot reaction mixture was poured into 200 ml ethanol. The precipitate was separated by centrifugation. Then, the product was repeatedly swollen in dichloromethane and precipitated in 5 volumes ethanol. Finally, the powdery products were thoroughly rinsed with ethanol.

Separation of microscaled cellulose fibers (M-CFS) from CFS

One hundred fifty mg CFS-1 or CFS-2 (Table 1) was dispersed in 10 ml tetrahydrofuran (THF) and treated with ultrasonication for 1 h at 0 °C. Then, the CFS-1 or CFS-2 suspension was centrifuged for 20 min at 5,000 rpm at 20 °C. After the centrifugation, the sediment and supernatant were separated. Due to different sizes and dispersing capabilities, the nano-scaled fragments stayed in THF, while the microscaled fibers sedimented during the centrifugation. The sediments were collected and dried, leading to M-CFS-1 and M-CFS-2, respectively.

Formation of (super)hydrophobic surfaces

The CFS or M-CFS powders were dispersed in THF and underwent further ultrasonication treatment at 0 °C in ice-water mixture for 1 h, leading to homogeneous CFS or M-CFS suspensions. Then, the suspensions were added to the acetone. After the removal of solvents, the separated CFS or M-CFS was dispersed again in acetone and underwent 5 min ultrasonication treatment. (Super)hydrophobic surfaces were obtained after the deposition of CFS or M-CFS suspensions on substrates, e.g., a silicon wafer, using the solvent-casting technique. In the meantime, the CFS-1 suspension in THF was also dried directly on a substrate as control (CFS-1-THF). Moreover, a surface using a composite of CFS-1 and polystyrene (PS) (95/5, w/w) was fabricated after the precipitation of their mixture in THF into methanol and following solvent casting. To check the thermostability, the superhydrophobic surfaces of CFS were treated in an oven at 80 °C for 15 min and then cooled down for the water contact angle measurement.

Table 1 Characters of surface-hydrophobized cellulose fibers

Samples	Starting material	DS[a]	Yield (wt%)	Crystallinity[b]
MCC	–	–	–	0.88
CFS-1	MCC	0.32	99.4	0.76
M-CFS-1	MCC	0.25	84.6	0.86
Cotton linters	–	–	–	0.57
CFS-2	Cotton linters	0.41	99.5	0.81
M-CFS-2	Cotton linters	0.3	91.4	0.76

MCC microcrystalline cellulose

[a] Determined by elemental analysis

[b] Determined via solid-state CP/MAS ^{13}C NMR spectroscopy. The deviations are all lower than 5 %

Characterization

Elemental analysis

The contents of carbon, hydrogen and nitrogen were determined with the Elemental Analyser vario EL III CHN from Elementar (Hanau, Germany). The total degree of substitution ascribed to stearoyl groups (DS_{SE}) was calculated according to Vaca-Garcia et al. (2001).

FT Raman spectroscopy

FT Raman spectra of the samples in small aluminium discs were recorded on a Bruker MultiRam spectrometer (Bruker Optics, Ettlingen, Germany) with a Ge diode as detector that is cooled with liquid nitrogen. A cw-Nd:YAG laser with an exciting line of 1,064 nm was applied as light source for the excitation of Raman scattering. The spectra were recorded over 3,500–150 cm^{-1} using an operating spectral resolution of 3 cm^{-1} and a laser power output of 100 mW. A double analysis per 200 scans was carried out, and an average Raman spectrum was formed afterwards.

Solid-state CP/MAS ^{13}C NMR spectroscopy

Solid-state CP/MAS ^{13}C NMR spectroscopy was performed on a Bruker Avance II+400 WB spectrometer (Bruker Biospin, Ettlingen, Germany) at room temperature (RT) with a ^{13}C frequency of 400 MHz, 10 kHz spinning speed, 5 ms contact time and ^{1}H decoupling of 20 tppm.

Scanning electron microscopy (SEM)

Scanning electron microscopy (SEM) images were obtained on a Philips XL30 FEG high-resolution scanning electron microscope (HR-SEM) (FEI Deutschland GmbH, Frankfurt/Main, Germany). A 10-nm layer of platinum/palladium was coated on the surface of samples before SEM measurements.

Atomic force microscopy (AFM)

An MFP-3D system (Asylum Research, Santa Barbara, CA, USA) was used for AFM imaging in noncontact mode using cantilevers with resonance frequencies of approximately 150 kHz and a nominal force constant of 5 N/m (BudgetSensors, Innovative Solutions Bulgaria, Ltd., Sofia, Bulgaria) at a scan speed of 10 μm/s. The program IGOR Pro 6.22A (WaveMetrics Inc., Lake Oswego, OR, USA) was used to guide the AFM measurements and Gwyddion (Free Software Foundation, Inc., Boston, MA, USA) for the analysis of AFM images, respectively.

Static, advancing and receding water contact angle

Static contact angles of water drops of 4 μl on surfaces were measured using Contact Angle System OCA 15EC (Dataphysics, Filderstadt, Germany) at RT. Advancing and receding contact angles were measured by the sessile drop technique with Drop Shape Analysis System DSA100 (Krüss GmbH, Hamburg, Germany) by inflating or deflating the drop on the surfaces.

Drop impact experiments

Water drops of ~10 μl were released from a height of 2 cm above the surfaces. A cold light source with a diffuser was used to illuminate the drop and surface from the backside. The impact process was recorded by a high-speed video camera (FASTCAM SA-1, Photron Inc., USA) with 5,000 fps.

Results and discussion

Surface-hydrophobized cellulose fibers

The general strategy of the present work is to use surface-hydrophobized cellulose fibers for the construction of superhydrophobic surfaces (Scheme 1). Surface-hydrophobized cellulose fibers by stearoyl groups (CFS) were obtained after the partial esterification of the cellulose fiber surface under heterogeneous conditions. FT Raman spectra of the obtained products confirmed the introduction of stearoyl groups based on their characteristic bands at 2,851, 1,439 and 1,297 cm^{-1} (Fig. 1a). The average degree of substitution (DS) ascribed to stearoyl groups was determined to be around 0.4 (Table 1). Solid-state CP/MAS ^{13}C NMR spectra not only confirmed the introduction of stearoyl groups, but also showed the typical signals attributed to the crystalline region of cellulose (Fig. 1b). Based on the signals ascribed to crystalline (88.9 ppm) and amorphous (84.2 ppm) regions of cellulose, the crystallinities were determined (Table 1) (Larsson et al. 1997; Park et al. 2009; Teeäär et al. 1987). Thus, obtained surface-hydrophobized cellulose fibers contained crystalline cores, while only the surface was esterified by stearoyl groups.

After the synthesis, the product contained two main components: surface-hydrophobized cellulose microfibers (M-CFS) and nanoscaled fragments. These two components could be separated via centrifugation at 5,000 rpm for 20 min. The bigger microfibers representing the major component of the product (>80 wt%) sedimented at the bottom, while the nanoscaled fragments stayed in the supernatant (Table 1). SEM measurement showed aggregated nanoscaled fragments from MCC (Fig. 2a) during the drying process (Fig. 2b). Thus, AFM technique was applied for the illustration. The nanoscaled fragments exhibited a diameter of 20–40 nm and a length of 0.3–1 μm (Fig. 2c, d). The presence of microfibers as major component was due to the step-wise modification of cellulose fibers under heterogeneous conditions, which generally began from the surface and extended to the core (Berlioz et al. 2009). The cellulose type as MCC or cotton linters did not strongly affect the reaction between the stearic chloride and hydroxyl groups of cellulose based on similar degrees of substitution (DSs) of CFSs (Table 1). By using cotton linters, slightly higher DS and higher yield of microfibers were obtained compared to microcrystalline cellulose. While 84.6 % microfibers were obtained after the surface-modification of microcrystalline cellulose (MCC), 91.4 % microfibers were found by using larger cotton linter cellulose fibers. This fact is probably due to the bigger size of cotton linters compared to that of MCC (granule size of 50 μm); thus, fewer nanoscaled segments were synthesized. This

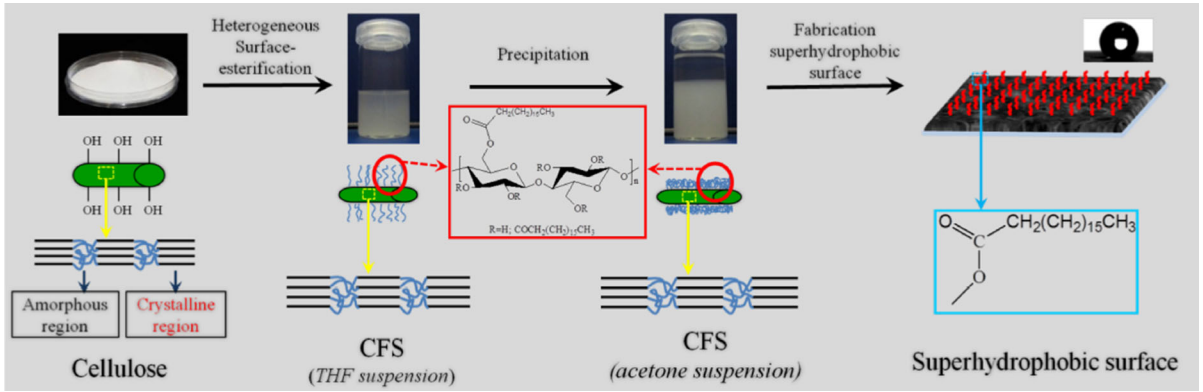

Scheme 1 Schematic illustration of the synthesis of surface-hydrophobized cellulose fibers for the construction of superhydrophobic surfaces. *CFS* cellulose fibers with surface-attached stearoyl groups

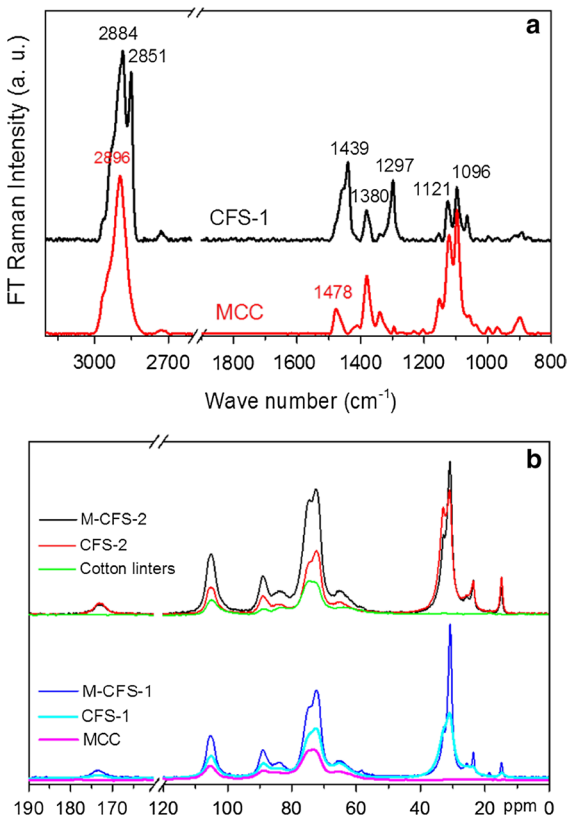

Fig. 1 **a** FT Raman spectrum of MCC and CFS-1. **b** Solid-state CP/MAS ^{13}C NMR spectra of cellulose and CFS-1/2 as well as M-CFS-1/2. *CFS* cellulose fibers with surface-attached stearoyl groups, *M-CFS* microscaled cellulose fibers separated from CFS

was also reflected by the crystallinity change for both celluloses. MCC exhibits a crystallinity of 88 %, and CFS-1 from MCC shows a slightly lower crystallinity of 76 %. In comparison, the major component M-CFS-1 has a higher crystallinity of 86 %, indicating that the other components in CFS-1 are more disordered. In comparison to MCC, the starting cotton linter fibers have a low crystallinity of only 57 %. However, the crystallinity of CFS-2 increased strongly to 81 %, and M-CFS-2 exhibited a crystallinity of 76 %, implying that the disordered regions should have been modified into soluble cellulose derivatives and removed during the purification with THF. Thus, only highly crystalline, surface-modified microfibers were obtained.

Obtained surface-hydrophobized cellulose fibers cannot be dissolved by the common organic solvents because of the presence of the crystalline cellulose matrix, but can be well dispersed in THF, dichloromethane or toluene because of the presence of stearoyl groups on the fiber surfaces (Scheme 1) (Lee et al. 2014; Klemm et al. 2005).

(Super)hydrophobic surfaces

(Super)hydrophobic surfaces were fabricated by depositing modified cellulose fibers from their suspensions via diverse routes, e.g., solvent casting, spin coating or spray coating. Directly depositing CFS from its THF suspension only led to hydrophobic surfaces showing a static water contact angle of 122 ± 1° (Fig. 3). Probably, the direct deposition of CFS from THF resulted in a smooth surface because of the strong interaction between stearoyl groups and THF (Fig. 4a). Thus, acetone was used as a suspension medium for CFS and M-CFS, while methanol was used only for composites containing polystyrene

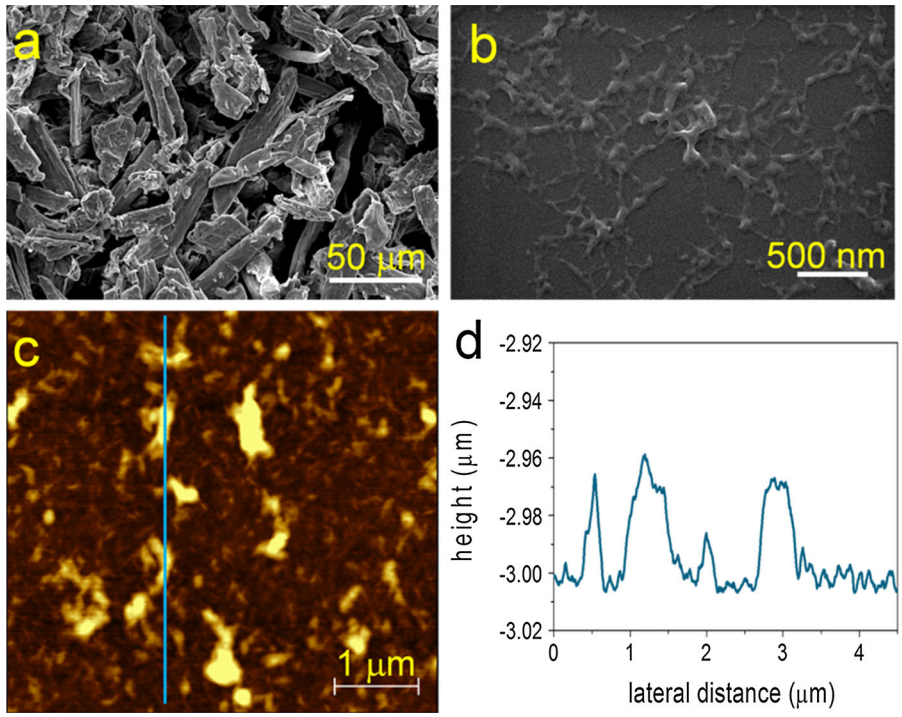

Fig. 2 **a** A representative SEM image of microcrystalline cellulose (MCC) with a scale bar of 50 μm; **b** a representative SEM image of nanoscaled fragments separated from CFS-1 with a scale bar of 500 nm; **c** a representative AFM image of nanoscaled fragments as a minor component in the supernatant after the separation of microsized M-CFS. *Scale bar* 1 μm; **d** the height profile measured at the positions as indicated by the blue line in (**c**)

(5 wt %) because of the solubility of polystyrene in acetone. After the deposition, superhydrophobic surfaces showing a static water contact angle of >150° were obtained (Fig. 3). The surface from both CFS-1 and CFS-2 exhibited similar static contact angles.

Furthermore, surfaces from sole M-CFS were only hydrophobic and showed static water contact angles between 130 and 145° (Fig. 3). In comparison to surfaces from freshly prepared CFS-1/2 containing nanoscaled fragments, the surfaces from M-CFS are composed of microfibers (Figs. 4, 5). Without the nanoscaled fragments, the surface roughness based on these microfibers is probably not sufficient for the superhydrophobicity, so water still can penetrate between microfibers (Dorrer and Rühe 2009). In contrast, nanoscaled segments or polystyrene could fill the space between the microfibers and thus contribute further to the hydrophobicity (Figs. 4b, 5b). Polystyrene could even form nanoparticles on the surface of cellulose microfibers (Fig. 4d).

Water droplet impact on diverse surfaces was analyzed in order to better understand the surface properties (Fig. 6) (Chen et al. 2011). It is visible that water droplets pinned onto the surfaces from CFS-1, M-CFS-1 and M-CFS-2, while water droplets bounced off the surfaces from CFS-1-PS and CFS-2 (Fig. 6). In the droplet impact testing, the wetting pressure (effective water hammer pressure and dynamic pressure) and antiwetting pressure (capillary pressure) played dominant roles (Deng et al. 2009; Chen et al. 2010). Regarding CFS-1-PS and CFS-2, the presence of polystyrene nanoparticles and nanoscaled fragments decreased the size of the voids on the surfaces, leading to a higher capillary pressure. Subsequently, water drops could completely rebound off and the surface stayed nonwetting (Chen et al. 2010). For CFS-1, M-CFS-1 and M-CFS-2 with a lower capillary pressure caused by the large voids on the surfaces, droplets can overcome the Cassie-Wenzel free energy barrier and result in wetting of the surfaces (Koishi et al. 2009). Moreover, a threshold impact velocity exists that dominates the droplet rebounding or staying on the surfaces in the droplet impact test (Reyssat et al. 2006). Normally, smaller contact angle hysteresis causes smaller threshold impact velocity, indicating more hydrophobic surfaces (Chen et al. 2010). Thus, the contact angle hysteresis of the three superhydrophobic surfaces from CFS-1, CFS-1-PS and CSF-2 was then further studied (Fig. 7). Although they all showed advancing angles of >160°, the surfaces from CFS-1-PS and CFS-2 showed significantly higher

receding angles and thus lower contact angle hysteresis. These results confirmed again that the surfaces fabricated from sole M-CFS are more adhesive to water than the surfaces fabricated using CFS-1/2 containing nanoscaled fragments. Furthermore, the surfaces from CFS-2 showed less interaction with water during impact analysis than surfaces from CFS-1, which indicates on the one hand fewer defect sites and on the other hand a more stable superhydrophobic surface. In comparison to CFS-1 from MCC, CFS-2 from cotton linters has a slightly higher DS and thus higher surface coverage by stearoyl groups. Thus, the CFS-2 surface possesses fewer accessible sites for water to interact with, which contributes to the construction of superhydrophobic surfaces.

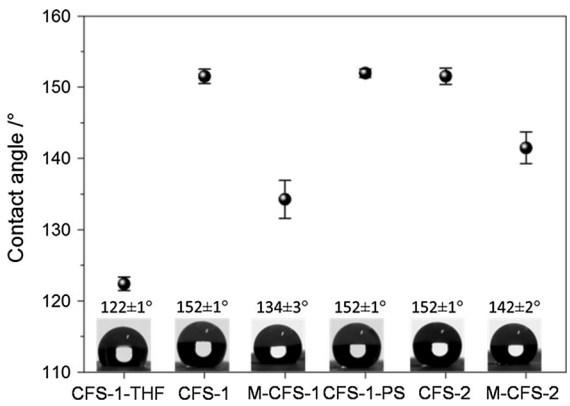

Fig. 3 Static water contact angles on diverse surfaces from surface-hydrophobized cellulose fibers (CFS-1-THF: surfaces deposited from the THF-suspension of CFS-1; CFS-1-PS: surfaces deposited from the methanol suspension of CFS-1 and polystyrene; the other surfaces deposited from their acetone suspensions)

The superhydrophobic surfaces were further analyzed regarding their thermostability (Fig. 7). The interactions between alkyl groups are generally not stable at high temperature so that the crystalline regions formed by stearoyl groups can be destructed, e.g., at 70 °C (Sealey et al. 1996; Vaca-Garcia et al. 2003). As reported previously, the superhydrophobic layers based on nanoparticles of cellulose stearoyl esters were transformed into hydrophobic ones following a treatment at 70 °C for 5 min (Geissler et al. 2014). In comparison, the superhydrophobic surfaces based on surface-hydrophobized cellulose microfibers, e.g., from CFS-1-PS and CFS-2, are stable during the heat treatment, e.g., at 80 °C for 15 min (Fig. 7). Only the surface from CFS-1 became slightly less hydrophobic after the heat treatment at 80 °C for 15 min. The stability against the heat treatment at 80 °C is attributed to the presence of crystalline cellulose microfibers, which were maintained during the treatment (Klemm et al. 2005; Atalla and Vanderhart 1984). In contrast, many synthetic polymers and cellulose derivatives, such as cellulose stearoyl esters, undergo a melting process at high temperatures (Geissler et al. 2014; Vaca-Garcia et al. 2003; Sealey et al. 1996). Following the treatment, the nano-/microscale surface roughness contributing to the superhydrophobicity will be eliminated. In comparison, superhydrophobic surfaces using a crystalline

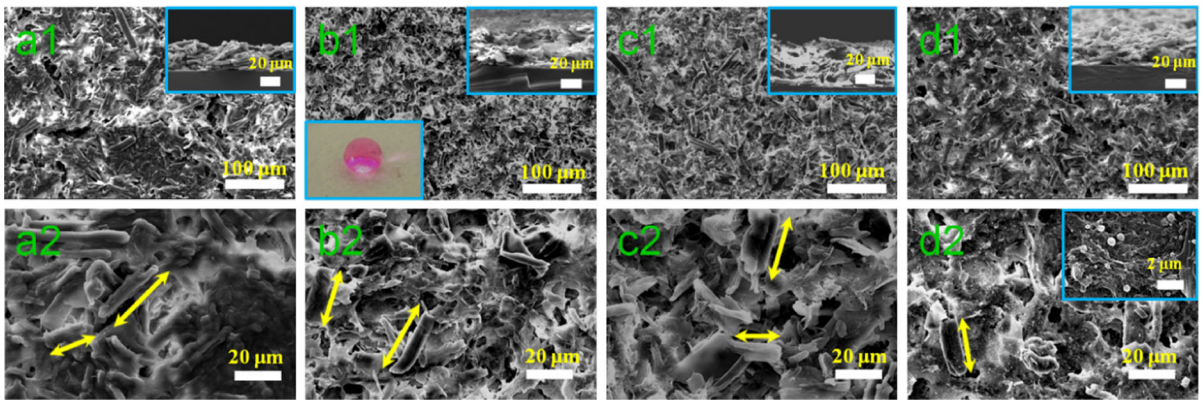

Fig. 4 SEM images of surfaces from **a** CFS-1-THF, **b** CFS-1, **c** M-CFS-1 and **d** CFS-1-PS. *Scale bar* in 1: 100 µm and in 2: 20 µm. *Insets* in **a1–d1** are side profiles of the surfaces with a *scale bar* of 20 µm; the other *inset* in **b1** shows the photo of a water droplet dyed with rhodamine on the surface from CFS-1; the *inset* in **d2** shows polystyrene nanoparticles on the surface of cellulose microfibers with a *scale bar* of 2 µm. The *arrows* indicate whole microfibers

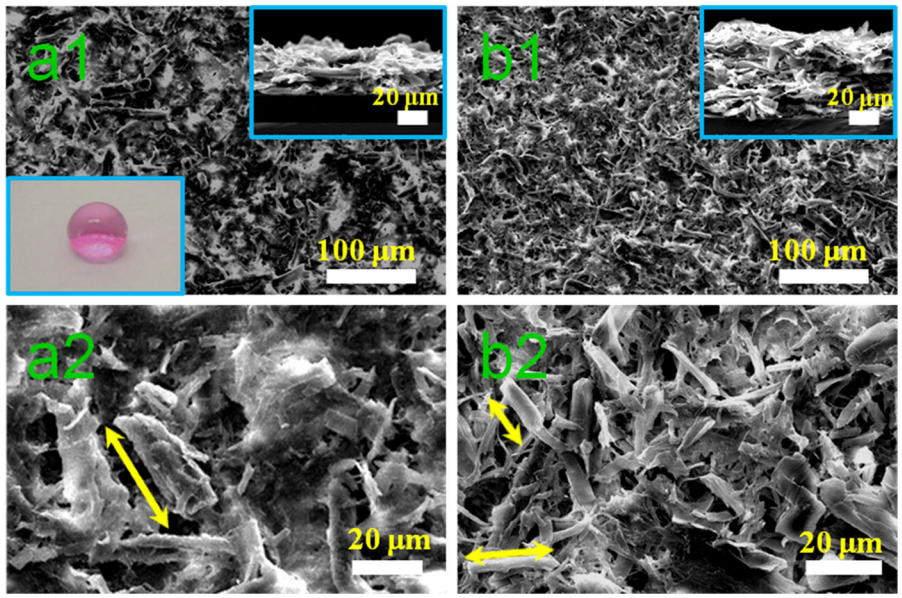

Fig. 5 SEM images of surfaces from **a** CFS-2 and **b** M-CFS-2. *Scale bar* in 1: 100 μm and in 2: 20 μm. *Insets* in **a1** and **b1** are side profiles of the surfaces with *scale bar* of 20 μm. The other *inset* in **a1** shows the photograph of a water droplet dyed with rhodamine on the surface of CFS-2. The *arrows* indicate whole microfibers

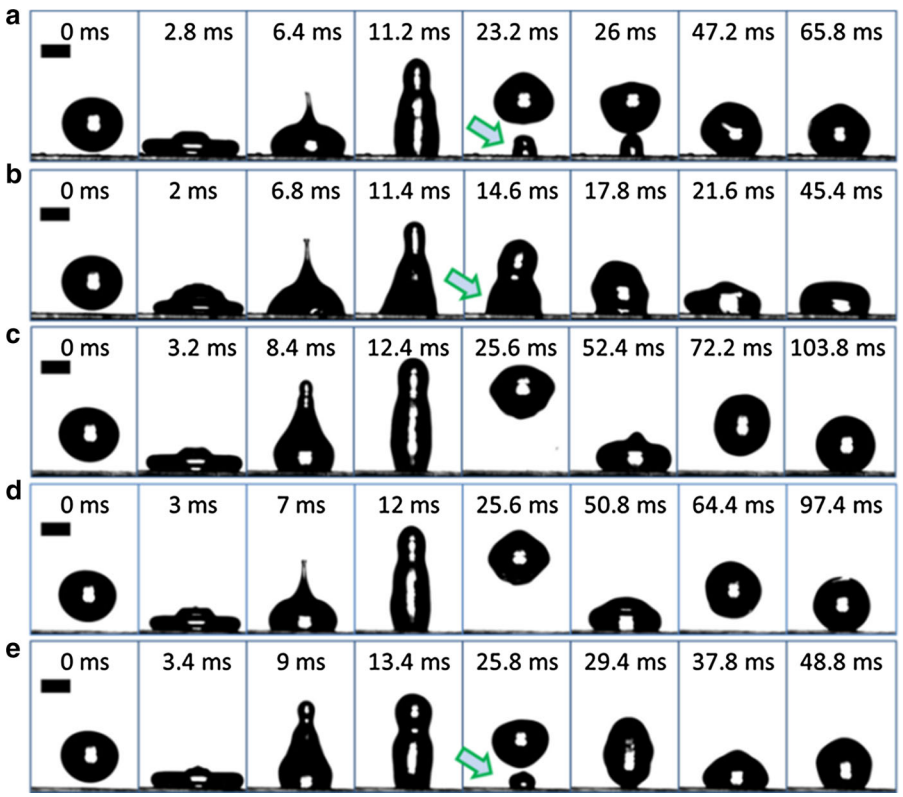

Fig. 6 Snapshots of water drop impact experiments on the surfaces prepared with **a** CFS-1, **b** M-CFS-1, **c** CFS-1-PS, **d** CFS-2 and **e** M-CFS-2. *Scale bar* 2 μm. The *arrows* indicate the pinning of water drops on surfaces

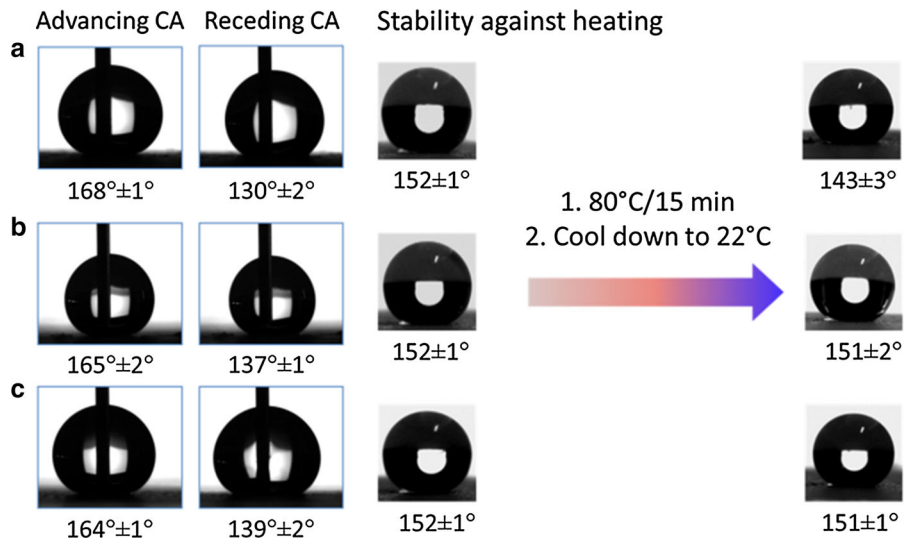

Fig. 7 Advancing, receding angles as well as static contact angles before and after the heat treatment of superhydrophobic surfaces from **a** CFS-1, **b** CFS-1-PS and **c** CFS-2

cellulose skeleton as the construction material are more stable during the high temperature treatment.

Conclusion

In summary, we showed in this study the feasibility of using surface-hydrophobized cellulose fibers (CFS) for the construction of (super)hydrophobic surfaces. The surface of cellulose fibers was decorated with stearoyl groups, which endow the cellulose fibers with hydrophobicity. The final product after the synthesis contains two components: surface-hydrophobized cellulose microfibers as a major component and nanoscaled fragments in small amounts. The crystalline cellulose structure was maintained according to solid-state ^{13}C NMR spectroscopy. Superhydrophobic surfaces were obtained by using freshly prepared products containing both components via facile route, e.g., solvent casting. The superhydrophobic surfaces showed a static water contact angle of more than 150°. In comparison, surface-hydrophobized cellulose microfibers (M-CFS) were solely constructed hydrophobic surfaces. Hydrophobized cellulose fibers could also be used together with other hydrophobic polymers including polystyrene in order to improve the superhydrophobic surface property by combining the microstructure of cellulose fibers and nanostructure of polystyrene. Due to the presence of the crystalline cellulose skeleton, the obtained superhydrophobic surfaces are stable against treatments at 80 °C.

Acknowledgments Authors thank the Hessian excellence initiative LOEWE Research Cluster SOFT CONTROL for the financial support. We thank Prof. M. Biesalski for the kind support. Y.W. thanks the CSC (Chinese Scholarship Council) for financial support.

References

Atalla RH, Vanderhart DL (1984) Native cellulose: a composite of two distinct crystalline forms. Science 223(4633): 283–285. doi:10.1126/science.223.4633.283

Azimi G, Dhiman R, Kwon HM, Paxson AT, Varanasi KK (2013) Hydrophobicity of rare-earth oxide ceramics. Nat Mater 12(4):315–320. doi:10.1038/nmat3545

Barthlott W, Neinhuis C (1997) Purity of the sacred lotus, or escape from contamination in biological surfaces. Planta 202(1):1–8. doi:10.1007/s004250050096

Bayer IS, Fragouli D, Attanasio A, Sorce B, Bertoni G, Brescia R, Di Corato R, Pellegrino T, Kalyva M, Sabella S, Pompa PP, Cingolani R, Athanassiou A (2011) Water-repellent cellulose fiber networks with multifunctional properties. ACS Appl Mater Inter 3(10):4024–4031. doi:10.1021/am200891f

Berlioz S, Molina-Boisseau S, Nishiyama Y, Heux L (2009) Gas-phase surface esterification of cellulose microfibrils and whiskers. Biomacromolecules 10(8):2144–2151. doi:10.1021/bm900319k

Caschera D, Mezzi A, Cerri L, Caro T, Riccucci C, Ingo GM, Padeletti G, Biasiucci M, Gigli G, Cortese B (2013) Effects of plasma treatments for improving extreme wettability behavior of cotton fabrics. Cellulose 21(1):741–756. doi:10.1007/s10570-013-0123-0

Chen LQ, Xiao ZY, Chan PCH, Lee YK (2010) Static and dynamic characterization of robust superhydrophobic surfaces built from nano-flowers on silicon micro-post arrays. J Micromech Microeng 20(10). doi:10.1088/0960-1317/20/10/105001

Chen L, Xiao Z, Chan PCH, Lee Y-K, Li Z (2011) A comparative study of droplet impact dynamics on a dual-scaled superhydrophobic surface and lotus leaf. Appl Surf Sci 257(21):8857–8863. doi:10.1016/j.apsusc.2011.04.094

Clift MJ, Foster EJ, Vanhecke D, Studer D, Wick P, Gehr P, Rothen-Rutishauser B, Weder C (2011) Investigating the interaction of cellulose nanofibers derived from cotton with a sophisticated 3D human lung cell coculture. Biomacromolecules 12(10):3666–3673. doi:10.1021/bm200865j

Cunha AG, Freire CS, Silvestre AJ, Pascoal Neto C, Gandini A, Orblin E, Fardim P (2007) Highly hydrophobic biopolymers prepared by the surface pentafluorobenzoylation of cellulose substrates. Biomacromolecules 8(4):1347–1352. doi:10.1021/bm0700136

Deng T, Varanasi KK, Hsu M, Bhate N, Keimel C, Stein J, Blohm M (2009) Nonwetting of impinging droplets on textured surfaces. Appl Phys Lett 94(13). doi:10.1063/1.3110054

Deng X, Mammen L, Butt HJ, Vollmer D (2012) Candle soot as a template for a transparent robust superamphiphobic coating. Science 335(6064):67–70. doi:10.1126/science.1207115

Dorrer C, Rühe J (2008) Wetting of silicon nanograss: from superhydrophilic to superhydrophobic surfaces. Adv Mater 20(1):159–163. doi:10.1002/adma.200701140

Dorrer C, Rühe J (2009) Some thoughts on superhydrophobic wetting. Soft Matter 5(1):51. doi:10.1039/b811945g

Erbil HY, Demirel AL, Avci Y, Mert O (2003) Transformation of a simple plastic into a superhydrophobic surface. Science 299(5611):1377–1380. doi:10.1126/science.1078365

Feng XJ, Jiang L (2006) Design and creation of superwetting/antiwetting surfaces. Adv Mater 18(23):3063–3078. doi:10.1002/adma.200501961

Feng L, Li SH, Li YS, Li HJ, Zhang LJ, Zhai J, Song YL, Liu BQ, Jiang L, Zhu DB (2002) Super-hydrophobic surfaces: from natural to artificial. Adv Mater 14(24):1857–1860. doi:10.1002/adma.200290020

Gao X, Jiang L (2004) Biophysics: water-repellent legs of water striders. Nature 432(7013):36. doi:10.1038/432036a

Geissler A, Biesalski M, Heinze T, Zhang K (2014) Formation of nanostructured cellulose stearoyl esters via nanoprecipitation. J Mater Chem A 2(4):1107. doi:10.1039/c3ta13937a

Genzer J, Efimenko K (2000) Creating long-lived superhydrophobic polymer surfaces through mechanically assembled monolayers. Science 290(5499):2130–2133. doi:10.1126/science.290.5499.2130

Guo Z, Zhou F, Hao J, Liu W (2005) Stable biomimetic superhydrophobic engineering materials. J Am Chem Soc 127(45):15670–15671. doi:10.1021/ja0547836

He M, Xu M, Zhang LN (2013) Controllable Stearic Acid Crystal Induced High Hydrophobicity on Cellulose Film Surface. ACS Appl Mater Inter 5(3):585–591. doi:10.1021/Am3026536

Heux L, Chauve G, Bonini C (2000) Nonflocculating and chiral-nematic self-ordering of cellulose microcrystals suspensions in nonpolar solvents. Langmuir 16(21):8210–8212. doi:10.1021/La9913957

Jin C, Jiang Y, Niu T, Huang J (2012) Cellulose-based material with amphiphobicity to inhibit bacterial adhesion by surface modification. J Mater Chem 22(25):12562. doi:10.1039/c2jm31750h

Klemm D, Heublein B, Fink HP, Bohn A (2005) Cellulose: fascinating biopolymer and sustainable raw material. Angew Chem Int Ed Engl 44(22):3358–3393. doi:10.1002/anie.200460587

Koishi T, Yasuoka K, Fujikawa S, Ebisuzaki T, Zeng XC (2009) Coexistence and transition between Cassie and Wenzel state on pillared hydrophobic surface. Proc Natl Acad Sci USA 106(21):8435–8440. doi:10.1073/pnas.0902027106

Larsson PT, Wickholm K, Iversen T (1997) A CP/MAS ^{13}C NMR investigation of molecular ordering in celluloses. Carbohydr Res 302:19–25

Lee KY, Blaker JJ, Murakami R, Heng JY, Bismarck A (2014) Phase behavior of medium and high internal phase water-in-oil emulsions stabilized solely by hydrophobized bacterial cellulose nanofibrils. Langmuir 30(2):452–460. doi:10.1021/la4032514

Li S, Xie H, Zhang S, Wang X (2007) Facile transformation of hydrophilic cellulose into superhydrophobic cellulose. Chem Comm 46:4857. doi:10.1039/b712056g

Li G, Zheng H, Wang Y, Wang H, Dong Q, Bai R (2010) A facile strategy for the fabrication of highly stable superhydrophobic cotton fabric using amphiphilic fluorinated triblock azide copolymers. Polymer 51(9):1940–1946. doi:10.1016/j.polymer.2010.03.002

Malmström E, Carlmark A (2012) Controlled grafting of cellulose fibres—an outlook beyond paper and cardboard. Polym Chem 3(7):1702. doi:10.1039/c1py00445j

Nystrom D, Lindqvist J, Ostmark E, Hult A, Malmstrom E (2006) Superhydrophobic bio-fibre surfaces via tailored grafting architecture. Chem Commun 34:3594–3596. doi:10.1039/b607411a

Park S, Johnson DK, Ishizawa CI, Parilla PA, Davis MF (2009) Measuring the crystallinity index of cellulose by solid state 13C nuclear magnetic resonance. Cellulose 16(4):641–647. doi:10.1007/s10570-009-9321-1

Reyssat M, Pepin A, Marty F, Chen Y, Quere D (2006) Bouncing transitions on microtextured materials. Europhys Lett 74(2):306–312. doi:10.1209/epl/i2005-10523-2

Roy D, Guthrie JT, Perrier S (2005) Graft Polymerization: grafting Poly(styrene) from cellulose via reversible addition—fragmentation chain transfer (RAFT) Polymerization. Macromolecules 38(25):10363–10372. doi:10.1021/ma0515026

Sealey JE, Samaranayake G, Todd JG, Glasser WG (1996) Novel cellulose derivatives. IV. Preparation and thermal analysis of waxy esters of cellulose. J Polym Sci Part B Polym Phys 34:1613–1620

Simončič B, Hadžić S, Vasiljević J, Černe L, Tomšič B, Jerman I, Orel B, Medved J (2013) Tailoring of multifunctional cellulose fibres with "lotus effect" and flame retardant properties. Cellulose 21(1):595–605. doi:10.1007/s10570-013-0103-4

Song JL, Rojas OJ (2013) Approaching super-hydrophobicity from cellulosic materials: a Review. Nord Pulp Pap Res J 28(2):216–238

Teeäär R, Serimaa R, Paakkarl T (1987) Crystallinity of cellulose, as determined by CP/MAS NMR and XRD methods. Polym Bull 17(3). doi:10.1007/bf00285355

Vaca-Garcia C, Borredon ME, Gaseta A (2001) Determination of the degree of substitution (DS) of mixed cellulose esters by elemental analysis. Cellulose 8(3):225–231. doi:10.1023/a:1013133921626

Vaca-Garcia C, Gozzelino G, Glasser WG, Borredon ME (2003) Dynamic mechanical thermal analysis transitions of partially and fully substituted chellulose fatty esters. J Polym Sci Part B Polym Phys 41:281–289

Vasiljević J, Gorjanc M, Tomšič B, Orel B, Jerman I, Mozetič M, Vesel A, Simončič B (2012) The surface modification of cellulose fibres to create super-hydrophobic, oleophobic and self-cleaning properties. Cellulose 20(1):277–289. doi:10.1007/s10570-012-9812-3

Vuoti S, Talja R, Johansson L-S, Heikkinen H, Tammelin T (2013) Solvent impact on esterification and film formation ability of nanofibrillated cellulose. Cellulose 20(5): 2359–2370. doi:10.1007/s10570-013-9983-6

Xu B, Cai Z (2008) Fabrication of a superhydrophobic ZnO nanorod array film on cotton fabrics via a wet chemical route and hydrophobic modification. Appl Surf Sci 254(18):5899–5904. doi:10.1016/j.apsusc.2008.03.160

Yu M, Gu G, Meng W-D, Qing F-L (2007) Superhydrophobic cotton fabric coating based on a complex layer of silica nanoparticles and perfluorooctylated quaternary ammonium silane coupling agent. Appl Surf Sci 253(7): 3669–3673. doi:10.1016/j.apsusc.2006.07.086